Eur. Phys. J. B **23**, 165–170 (2001)

THE EUROPEAN PHYSICAL JOURNAL B
EDP Sciences

Dimensional crossover of quantum interference effects in thin quasicrystalline Al-Cu-Fe films

T. Grenet[a] and F. Giroud

LEPES-CNRS, 25 avenue des Martyrs, BP 166, 38042 Grenoble Cedex 9, France

Received 16 February 2001 and Received in final form 20 June 2001

Abstract. We present a study of the electrical transport properties of thin i-Al-Cu-Fe films. We observe clear signatures of a dimensional crossover in the temperature and magnetic field dependence of the conductivity for films thinner that $\simeq 10^3$ Å. In particular for the thinnest sample the magnetoconductivity is strongly anisotropic, as is expected for the weak localisation contribution in two dimensions. These experiments show direct qualitative manifestations of the disorder induced quantum interference effects occurring in quasicrystals. Estimates of the electronic microscopic parameters are in accordance with those obtained in bulk samples. Their values and significance are discussed.

PACS. 71.23.Ft Quasicrystals – 73.20.Fz Weak or Anderson localisation

1 Introduction

Stable quasicrystals (QCs) display surprising electrical transport properties [1]. Icosahedral alloys such as i-Al-Cu-Fe, i-Al-Pd-Mn or i-Al-Pd-Re have very high resistivities (from 10^{+4} to $10^{+6}\mu\Omega$ cm at 4 K). I-Al-Pd-Re even exhibits a metal to insulator transition. This transition may be unique as it occurs in a highly ordered alloy of metals without a gap in the density of states at E_F (according to low temperature specific heat data). Several theoretical approaches have been developed to explain the peculiar transport properties observed (see Roche *et al.* and Mayou [1,2]). They rely on the specific atomic order of the QCs. However at low temperature, the T and magnetic field dependence $\delta\sigma(T,B)$ was found to be similar to the one of disordered systems. In particular, $\delta\sigma(T,B)$ of i-Al-Cu-Fe, i-Al-Pd-Mn and metallic i-Al-Pd-Re samples was successfully fitted using quantum interference effects (QIE) theories [3–9].

The QIE theories predict T and B dependent corrections to the electrical conductivity of metals, due to interference effects of electrons elastically scattered by the disorder. These theories were elaborated in the weak disorder limit and are expected to well describe small corrections to the conductivity of metals [10]. However in the case of the QCs, the electron states markedly differ from free electron states, σ is quite small and the relative variations $\delta\sigma(T,B)/\sigma$ are rather large. Thus in i-$Al_{70.5}Pd_{22}Mn_{7.5}$ one has $\delta\sigma(B)/\sigma = [\sigma(B) - \sigma(0)]/\sigma(0) \sim 25\%$ at low T [6]. In the case of i-Al-Cu-Fe, it was claimed that the whole T dependence of σ from low T up to 200 K is mainly due to QIE, implying a quantum correction at low T amounting at least 30–35% of σ(200 K) [9]. Thus it seems surprising that the QIE theories work so well in these alloys. Note however that due to the number of degrees of freedom available, performing complete QIE fits is a difficult task. Authors often get large error bars for the microscopic parameters extracted or consider different approaches which do not all give exactly the same results [9,11].

In this context it is interesting to further test the relevance of QIE in quasicrystals by looking for qualitative signatures of their occurrence. The study of thin films makes such a test possible. The QIE theory predicts different $\delta\sigma(T,B)$ dependences for 3D and 2D samples. In bulk samples $\delta\sigma(T)$ follows a $T^{1/2}$ law at low enough T for the inelastic scattering time (and thus the weak localisation part) to be saturated ($T < 1{-}2$ K), and $\delta\sigma(B)$ behaves like $B^{1/2}$ at intermediate fields. In thin films, one instead expects $\delta\sigma(T) \propto \mathrm{Ln}(T)$ and $\delta\sigma(B) \propto \mathrm{Ln}(B)$. Moreover a characteristic anisotropy of $\delta\sigma(B)$ should be observed, which does not exist in 3D samples.

An indication of a two dimensional regime in i-Al-Cu-Fe thin films was given in [12] based on the T dependence at low T of ion beam thinned samples. The aim of the present work is to study the conductivity of thin QC Al-Cu-Fe films and seek for a clear signature of the dimensional crossover as a function of the samples thickness in the T and B dependences of the conductivity. In Section 2 we recall the basic QIE contributions to σ and the criteria for the crossover, and in Section 3 we briefly describe the samples preparation and characterisation. We then present the experimental measurements (Sect. 4). Their quantitative analysis and discussion are given in Section 5. A preliminary account of this work was given in [13].

[a] e-mail: grenet@lepes.polycnrs-gre.fr

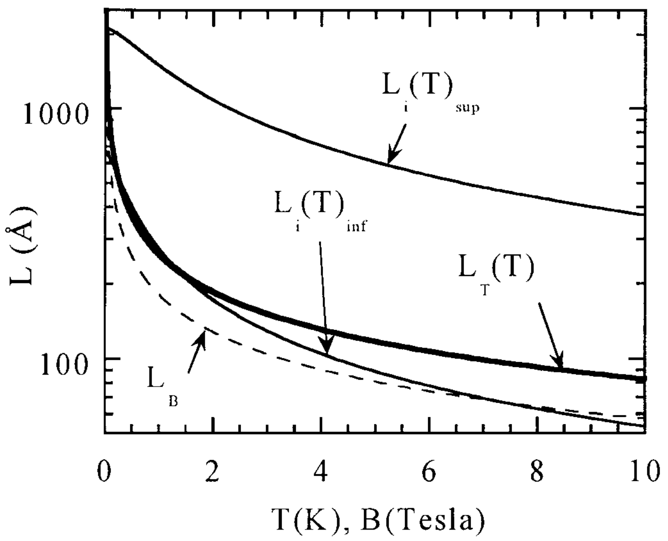

Fig. 1. Characteristic length governing the dimensional crossover of the quantum interference effects: $L_{\rm i}$ and L_T as a function of T, L_B as a function of B in tesla. We use $D = 0.3$ cm^2 s^{-1}, $L_{\rm i}(T)$ is estimated using the inferior and superior values of the scattering time given in [5].

2 Quantum interference effects and criteria for the dimensional crossover

As is well known the weak localisation contribution to $\delta\sigma(T,B)$ comes from the interference of time reversed closed loop path followed by the electrons. The inelastic scattering and an imposed magnetic field limit the size of the loops which effectively contribute to $\delta\sigma(T,B)$. A thin film is two dimensional for weak localisation if most of the coherent electron loop path are confined in the sample's plane. The following conditions must then be fulfilled: $L_{\rm i}(T) \gg t$ and $L_{\rm B} = (h/4\pi eB)^{1/2} \gg t$ (t is the film thickness, $L_{\rm i}(T)$ the inelastic mean free path and L_B the magnetic dephasing length). A second type of contribution arises from combined disorder scattering and electron-electron coulomb interaction (EEI contribution), the physical meaning of which has been discussed [14]. The coherence of the two electrons considered in this mechanism is limited by their energy difference of order $k_{\rm B}T$, and the magnetic field mostly acts *via* the Zeeman splitting, orbital effects on $\delta\sigma(B)$ being smaller. Then the criterion for a 2D EEI contribution is $L_T = (3hD/2\pi k_{\rm B}T)^{1/2} \gg t$ (D: electron diffusivity). Taking the values of D and $\tau_{\rm i}(T)$ deduced from the analysis of bulk i-Al-Cu-Fe samples, we can estimate below which range of temperature, magnetic field and film thickness the two dimensional effects should be observable. In Figure 1 we show the values of $L_{\rm i}(T)$, L_B and L_T estimated from the data of [6]. We conclude that below $T \sim 1$ K and $B \sim 1$ T, films a few hundred angstroms thick should be in the crossover region.

3 Sample preparation and characterisation

We made thin film samples of nominal composition $Al_{62.5}Cu_{25}Fe_{12.5}$ with thicknesses ranging from 9000 Å down to 125 Å. The samples were prepared by sequential evaporation of the chemical elements on sapphire substrates, followed by thermal treatments causing the interdiffusion and the growth of the quasicrystalline phase. The succession of phase transformations leading to pure quasicrystalline films was studied in detail [15,16]. We briefly describe the samples' characterisation which was presented in [13]. The flatness of the films is important for the present study. It was ensured by encapsulating the multilayers with alumina layers (500 Å or 1000 Å thick), which prevents the appearance of roughness during the annealings as checked by cross-sectional transmission electron microscopy. The quasicrystalline nature of the films and their phase purity was checked by grazing angle X-ray diffraction (XRD). However for the thinnest samples the diffraction signal is small and minority secondary phases could be present without being seen. The electrical conductivity of the films is then used as a complementary characterisation. It is indeed known that metallic secondary phases significantly increase the samples conductivities.

The $\sigma(T)$ of the samples studied here are shown in [13]. One has the same T dependence as that of bulk specimen, which is characteristic of quasicrystals and approximant phases. The absolute values of σ range from 300 to 500 (Ω cm)$^{-1}$ (at 4 K). They are thus higher than those of good quality bulk specimen (for which σ(4 K) ranges from 100 to 250 (Ω cm)$^{-1}$ [17]). This difference can in principle be due to a non-perfect crystallographic structure or to a non-optimum chemical composition of the QC phase [17], or to the presence of a conducting secondary phase. The diffraction peaks of thin films are indeed always broader than those of "perfect" bulk specimen. Moreover small composition differences can exist between the samples, as it becomes more difficult to control it in the thinnest films. However, no correlation is observed between the samples' thickness and their conductivity. Thus there seems to be no tendency for the thinner films to be of worse quality than the thicker ones which have clearly pure QC XRD spectra. The films in which the presence of secondary phases was observed by XRD all had higher conductivities than the samples studied here. We are thus confident that the properties of the films we study are characteristic of the QC phase.

The conductivity measurements at low temperature and in magnetic field were performed in a He^3 cryostat down to 0.45 K in the 1 tesla magnetic induction range, using the Van der Pauw contact geometry. For the anisotropy measurements, the samples were mounted on a orientable holder and could be rotated from parallel to perpendicular to the magnetic field inside the cryostat.

4 Experimental results

4.1 Temperature dependence of the conductivity at low T

The temperature dependence of σ was studied at low T as a function of the films thickness. In Figure 2 we show in a

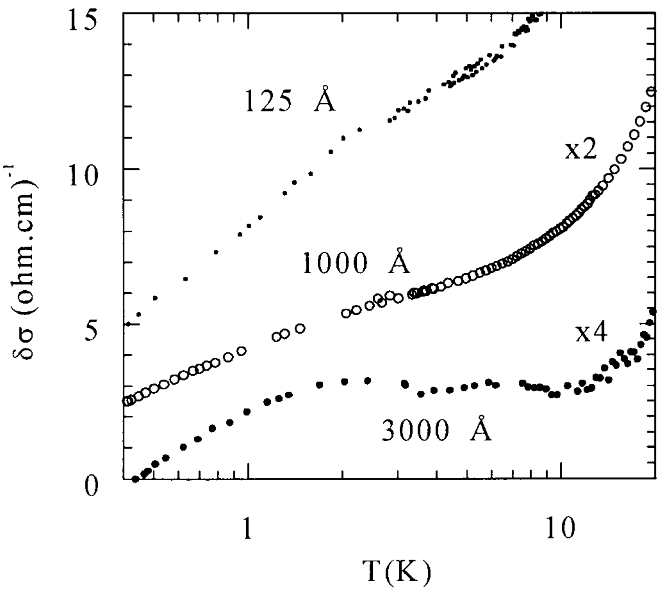

Fig. 2. Low temperature conductivity variations $\delta\sigma(T)$ for samples of thickness 3000 Å, 1000 Å and 125 Å. The curves are magnified and shifted for clarity.

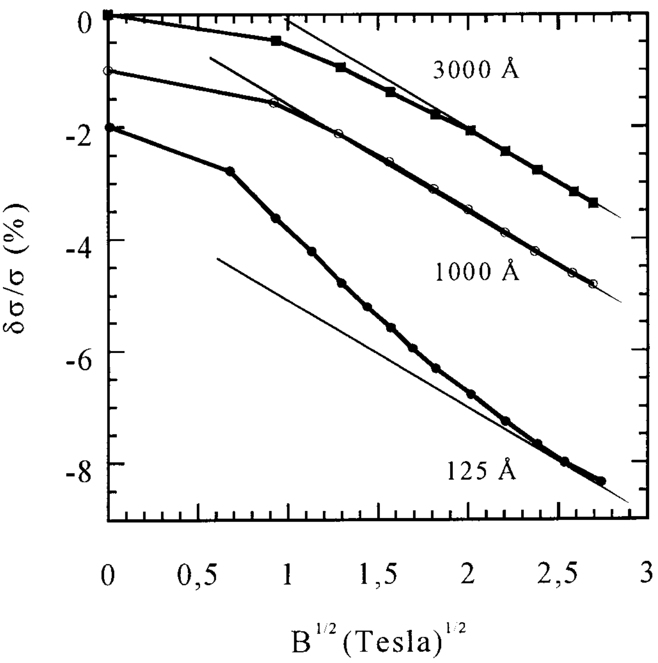

Fig. 3. Magnetoconductivity of 3000 Å, 1000 Å and 125 Å thick samples measured at $T = 0.5$ K. The straight lines are guides to show the change of curvature with the thickness.

semi-log scale the $\sigma(T)$ curves measured below $T = 10$ K for samples of thicknesses 3000 Å, 1000 Å and 125 Å. It is readily seen that whereas $\sigma(T)$ remains curved at the lowest T for the thickest sample, a $\mathrm{Ln}(T)$ dependence is observed for the 1000 Å and 125 Å samples, as expected for the 2D case.

4.2 Magnetoconductivity

We measured the magnetoconductivity of the films at low temperature. For the thicker samples the $\delta\sigma(B)/\sigma$ curves are very similar to the ones of the bulk i-Al-Cu-Fe samples [6]. However as the thickness decreases, the curvature of the magnetoconductivity curves changes. This is illustrated in Figure 3 where we compare the $\delta\sigma(B)/\sigma$ *versus* $B^{1/2}$ curves of the same samples of Figure 2 (B is parallel to the film plane).

At low field, a B^2 dependence is expected independently of the sample's dimensionality, whereas at higher fields (tesla range) $\delta\sigma(B) \sim \mathrm{Ln}(B)$ and $\delta\sigma(B) \sim (B)^{1/2}$ in 2D and 3D respectively. The change of curvature of $\delta\sigma(B)$ in the 125 Å corresponds nicely to the expected $B^2 \rightarrow \mathrm{Ln}(B)$ transition of a 2D film, whereas the thicker films all display a 3D behaviour ($B^2 \rightarrow (B)^{1/2}$). Thus the magnetoconductivity curves also show the dimensionality crossover in our series of samples. Unfortunately we cannot reliably fit the curves in the whole field range since, as shown in Figure 1, a 2D to 3D crossover is also expected in the 125 Å film when B is increased above a few tesla.

The best demonstration of the two dimensional regime is the appearance of an anisotropy in $\delta\sigma(B)$. In Figure 4 we show the $\delta\sigma(B)/\sigma$ curves at low T for the 125 Å sample for fields parallel and perpendicular to the film plane.

One observes a significant anisotropy (at $T = 0.45$ K, $\delta\sigma(B^{\perp})/\delta\sigma(B^{//}) \sim 2$ for $B \leq 0.2$ tesla) which diminishes as the field and the temperature are increased, as expected from weak localisation. Although signs of the dimensional cross-over were also observed in thicker samples as shown above, no significant anisotropy was observed in them. This point will be discussed below.

5 Quantitative analysis

In this section we fit the curves shown above with the expressions of 2D quantum interference effects. We will then compare the values of the microscopic parameters involved in the analysis with those obtained from 3D fits of bulk specimen measurements.

5.1 Fits of the curves

In the low field range considered here and at low temperature, the EEI contributions (spin and orbital effects) to the magnetoconductivity can be neglected and the curves were fitted using the weak localisation expressions only given in [18] in the strong spin-orbit limit ($1/\tau_{\mathrm{i}}(T) \ll 1/\tau_{\mathrm{so}}$). These expressions are valid in the diffusive regime (elastic mean free path l_{e} smaller than the film thickness) in the two-dimensional limit ($\min[L_{\mathrm{i}}(T), L_{\mathrm{B}}] \ll t$) but taking a finite film thickness into account for $\delta\sigma(B^{//})$. The diffusive limit is justified in our 125 Å thick film since estimates of the mean free path in quasicrystals give $l \sim 15-30$ Å [19]. We do not take the spin-flip rate $1/\tau_{\mathrm{s}}$ explicitly into account. Actually only a very small fraction of

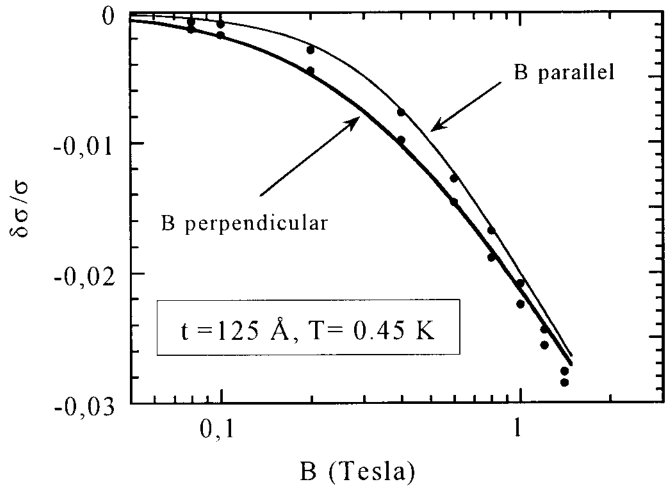

(a)

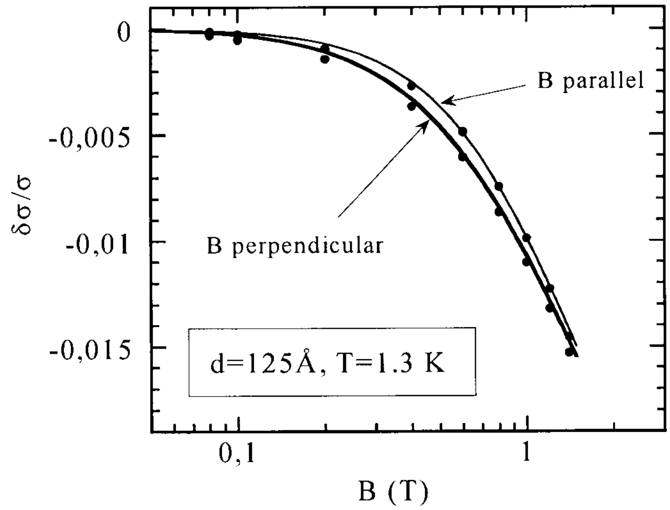

(b)

Fig. 4. (a) and (b) Magnetoconductivity in parallel and perpendicular fields at $T = 0.45$ K and $T = 1.3$ K for the 125 Å thick sample. The logarithmic scale is used to enhance the low field range. Dots are the experimental points and lines are the theoretical fits (see text).

the Fe atoms is magnetic in i-Al-Cu-Fe (10^{-5}–10^{-4} of the Fe atoms [20]). However at low temperature ($T < 1$ K)$1/\tau_s$ is not negligible compared to $1/\tau_i(T)$ (inelastic scattering rate). It is then implicitly included into the fitted scattering time. The fits are insensitive to the elastic scattering time, and the films thickness is known so that we have three free parameters: D, τ_{so} and $\tau_i(T)$.

The calculations show that $\tau_i(T)$ mostly influences the amplitude of $\delta\sigma(B)$ (beside the anisotropy), D influences the difference $\delta\sigma(B^{\perp}) - \delta\sigma(B^{\parallel})$ for a given $\tau_i(T)$, and τ_{so} changes the shape of the $\delta\sigma(B)$ curves. Thus as a first approximation we can estimate the three parameters independently. The four curves $(\delta\sigma(B^{\parallel,\perp})/\sigma$ at $T = 0.45$ K and $T = 1.3$ K) are of course fitted with the same values of D and τ_{so}, τ_i taking two values. The main uncertainties come from the one on τ_{so}. In Figure 4 we show the fits to $\delta\sigma(B)/\sigma$ for both field orientation at 0.45 K and 1.3 K, and see that quite good fits can be obtained. From these fits we estimate $D = 0.1 \pm 0.02$ cm^2 s^{-1}, $\tau_{so} = 2.5 \pm 1$ ps, $\tau_i(0.45\text{ K}) = 410 \pm 125$ ps and $\tau_i(1.3\text{ K}) = 110 \pm 30$ ps. The calculated curve ($T = 0.45$ K) start to deviate from the experimental points at $B \approx 1$ tesla. This is probably due to the neglect of EEI effects which start to contribute above one tesla, and to the proximity of the 2D to 3D transition induced by the field.

In principle one can also extract the screening parameter F_σ which governs the EEI contribution from $\delta\sigma(T)$. Combining both weak localisation and EEI effects the theory gives in 2D (in the limit $1/\tau_{so} \gg 1/\tau_i(T)$) [10]:

$$\sigma(T_2) - \sigma(T_1) = (e^2/\pi ht)\,[0.5\,\mathrm{Ln}(\tau_i(T_2)/\tau_i(T_1)) + (1 - 0.75\;F_\sigma)\;\mathrm{Ln}(T_2/T_1)]\,.$$

With only two values of $\tau_i(T)$ we can only roughly estimate F_σ. Assuming $1/\tau_i(T) \propto T^p$, we get $p \approx 1.23$ and $F_\sigma < 0.30$.

5.2 Discussion

Once we have values of the parameters we can check the consistency of our approximations. The calculated EEI contribution to $\delta\sigma(B)/\sigma$ is negligible, except when $T = 0.45$ K and $B > 1$ tesla where it amounts a few percent of the weak localisation part [21]. This can explain the deviation of the fit from the experimental points in that range. We also check that $L_B > (tL_i(T))^{1/2}$ so that a deviation from the 2D limit of $\delta\sigma(B^{//})/\sigma$ such as the one observed in [22] is not expected in our case. The high spin-orbit scattering limit ($\tau_{so} \ll \tau_i$) is also valid. Note that no significant anisotropy was observed with the 250 Å thick film. Indeed calculations show that, *even remaining in the 2D limit*, the anisotropy vanishes when "t" is increased since $|\delta\sigma(B^{\parallel})/\sigma|$ increases with "t". Moreover this film is more resistive that the 125 Å one and this also diminishes the anisotropy (effect of a smaller D).

We now compare our values of the fitting parameters to the ones obtained in bulk samples. A direct comparison is possible since the parameters D, τ_{so} and F_σ should take their 3D value in our films (l_e and the screening length are smaller than "t"). Dimensionality effects could reveal in the T dependence of $\tau_i(T)$ but we do not look for them. As our magnetoconductivity fits were performed in very limited T and B ranges (to stay in the 2D limit) we merely wish to compare the orders of magnitude of the parameters. Both $\tau_i(T)$ and τ_{so} are in the range of values obtained in bulk i-AlCuFe samples (see for instance [6]). As for D one generally fixes it to an estimated value in order to decrease the number of fitting parameters of full QIE fits. The difficulty in a priori estimating D is that it should not include the QIE effects. One uses the Einstein relation for σ and the values of $\sigma(T \sim 100$–300 K) for which QIE effects are negligible. This gives for bulk samples $D \approx 0.2$–0.3 cm^2 s^{-1} [6]. Applied to our 125 Å sample this procedure would give $D \approx 0.4–0.6$ cm^2 s^{-1}. But in our case D is a free parameter and we find $D \approx 0.1$ cm^2 s^{-1} from the fits. In fact it is not obvious that D has the same value at low T as at $T \sim 100–300$ K. Indeed σ increases continuously from the low T up to 1000 K without any change of regime or saturation [19] suggesting an equally increasing D. If so the diffusivity entering the QIE corrections at low T could be smaller than the $T \sim 100–300$ K estimate, which could at least partly explain the disagreement. Finally our estimate of the screening parameter ($F_\sigma < 0.30$) is also smaller than the previously published ones of bulk samples ($F_\sigma \sim 0.70–1.5$). This is consistent with the observation that it increases with the resistivity of the samples [9]. The authors of [9] have focused on its T dependence. However the significance of the values extracted from the fits is not clear. F_σ normally measures the static screening on the length $1/k_\mathrm{F}$ and depends on the electronic structure of the material. QIE fits including the EEI all use the spin-orbit free theory. The large spin-orbit scattering limit has been theoretically studied [23,24]. In that case the term of $\delta\sigma(T)$ proportional to F_σ vanishes, the magnetoconductance also decreases and becomes T independent. Unfortunately quasicrystals are in the intermediate regime. Indeed the broadening of the Zeeman levels is comparable to their splitting ($h/\tau_\mathrm{so} \sim g\mu_\mathrm{B}B$ for $B \sim 1$ T) and at low T (a few kelvin) one has $h/\tau_\mathrm{so} \sim k_\mathrm{B}T$. Thus in the fits F_σ is a phenomenological parameter which somehow takes into account the EEI contribution, but the meaning of its values is not clear as the theoretical expression for an arbitrary τ_so is not known.

The elastic scattering time τ_e is a very interesting parameter since it gives an insight into the transport mechanism in QCs. The perpendicular magnetoconductivity explicitly depends on τ_e, unfortunately due to the small values of D and B our fits are practically insensitive to it. One can estimate that if $l_\mathrm{e} \approx L_\mathrm{i}$ for $T \approx 100–300$ K then $l_\mathrm{e} \approx 20$ Å [19]. We also may try to get an estimate using τ_so, which characterises the carrier spin rotation upon the scattering on a defect. One expects $\tau_\mathrm{e} \approx (Z/137)^4\tau_\mathrm{so}$ [25]. The numerical factor containing Z is the probability of spin-flip during the elastic collision and Z is the atomic number associated to the defect. This relation was shown to hold in order of magnitude in different systems for the scattering on surfaces and impurities (Ref. [26] and Ref. [25] p. 327). In our case, assuming that the collisions mainly involve the transition elements (Fe and Cu) we get $\tau_\mathrm{e} \approx 2 \times 10^{-15\pm1}$ s corresponding to $l_\mathrm{e} \approx 0.8–8$ Å. This estimate is smaller than the ones based on $L_\mathrm{i}(T)$ and is also smaller than the typical size of the atomic clusters constituting the quasicrystals. Note that in their QIE study up to room temperature, Alghren *et al.* [9] also find a rather short elastic scattering time. It may suggest than the disorder as seen by the carriers is relatively important in QCs.

6 Conclusion

In summary, we have been able to make very thin Al-Cu-Fe QC films for the first time and study the influence of the thickness on their electrical conductivity. We have observed clear signatures of a 3D to 2D transition of the QIE contributions to $\sigma(T,B)$. Our observations (in particular the anisotropic magnetoconductivity) give direct qualitative illustrations of the occurrence of the QIE in the quasicrystal. It is seen that the QIE formula, although designed for the case of small corrections to σ, are also applicable to QCs in the 2D regime, and the values of the parameters are in accordance with the ones of bulk samples. Questions remain open about the extent to which the T dependence of σ can be explained solely by QIE, and about the importance and nature of the disorder seen by the carriers in QCs.

P.B. Barna, Z. Radi, A. Kovacs, G. Safran and J. Labar (RITPMS, Budapest) and A. Quivy (CECM, Vitry) are warmly thanked for the structural characterisation of the samples.

References

1. For review articles, see: C. Berger, in *From quasicrystals to more complex systems*, edited by F. Axel, F. Dénoyer, J.P. Gazeau (Springer-EDP Sciences, 2000); O. Rapp, in *Physical properties of quasicrystals*, edited by Z.M. Stadnik (Springer, 1999); T. Grenet, in *Quasicrystals Current Topics*, edited by E. Belin-Ferré, C. Berger, M. Quiquandon, A. Sadoc (World Scientific, 2000); S. Roche, G. Trambly de Laissardière, D. Mayou, J. Math. Phys. **38**, 1794 (1997); D. Mayou, in *Quasicrystals Current Topics*, edited by E. Belin-Ferré, C. Berger, M. Quiquandon, A. Sadoc (World Scientific, 2000).
2. C.V. Landauro, H. Solbrig, Mater. Sci. Eng. A **294-296**, 600 (2000).
3. T. Klein, H. Rakoto, C. Berger, G. Fourcaudot, F. Cyrot-Lackmann, Phys. Rev. B **45**, 2046 (1992).
4. A. Sahnoune, J.O. Ström-Olsen, A. Zaluska, Phys. Rev. B **46**, 10629 (1992).
5. R. Haberkern, G. Fritsch, J. Schilling, Z. Phys. B **92**, 383 (1993).
6. P. Lindqvist, P. Lanco, C. Berger, A.G.M. Jansen, F. Cyrot-Lackmann, Phys. Rev. B **51**, 4796 (1995).
7. M. Ahlgren, M. Rodmar, T. Klein, O. Rapp, Phys. Rev. B **51**, 7287 (1995).
8. T. Klein, O. Symko, C. Paulsen, Phys. Rev. B **51**, 12805 (1995).
9. M. Ahlgren, P. Lindqvist, M. Rodmar, O. Rapp, Phys. Rev. B **55**, 14847 (1997).
10. for review articles, see P.A. Lee, T.V. Ramakrishnan, Rev. Mod. Phys. **57**, 287 (1985); B.L. Altshuler, A.G. Aronov, in *Electron-electron interactions in disordered systems*, edited by A.L. Efros, M. Pollak (North Holland, 1985).
11. S. Matsuo, H. Nakano, K. Saito, M. Mori, T. Ishimasa, Solid State Comm. **86**, 707 (1993).
12. A. Yoshioka, K. Edagawa, S. Takeuchi, K. Kimura, Phys. Stat. Sol. B **201**, 97 (1997).
13. T. Grenet, F. Giroud, Mater. Sci. Eng. A **294-296**, 576 (2000).

14. G. Bergmann, Phys. Rev. B **35**, 4205 (1987).
15. T. Grenet, F. Giroud. C. Loubet, J.L. Joulaud, M. Capitan, Mater. Sci. Eng. A **294-296**, 838 (2000).
16. T. Grenet, F. Giroud, J.L. Joulaud, M. Capitan (submitted to Philosophical Magazine A).
17. T. Klein, C. Berger, D. Mayou, F. Cyrot-Lackmann, Phys. Rev. Lett. **66**, 2907 (1991).
18. S. Kobayashi, in *Localisation, Interaction and Transport Phenomena*, edited by B. Kramer, G. Bergmann, Y. Bruynseraede (Springer-Verlag, Berlin, 1985).
19. D. Mayou, C. Berger, F. Cyrot-Lackmann, T. Klein, P. Lanco, Phys. Rev. Lett. **70**, 3915 (1993).
20. R. Omari, Ph.D. thesis, Université Joseph Fourier, Grenoble, 1993.
21. We even overestimate the main (spin-splitting) EEI contribution to $\delta\sigma(B)$, since we use a spin-orbit free formula and the spin-orbit coupling is expected to reduce its magnitude.
22. C. McFadden, D.J. Newson, M. Pepper, N.J. Mason, J. Phys. C **18**, L383 (1985); D.J. Newson, M. Pepper, J. Phys. C **18**, L1049 (1985).
23. B.L. Altshuler, A.G. Aronov, Solid State Comm. **46**, 429 (1983).
24. A.J. Millis, P.A. Lee, Phys. Rev. B **30**, 6170 (1984).
25. V.F. Gantmakher, Y.B. Levinson, in *Carrier Scattering in Metals and Semiconductors* (North Holland, 1987).
26. R. Meservey, P.M. Tedrow, Phys. Rev. Lett. **41**, 805 (1978).